

Four-Body Calculation of Proton- ^3He Scattering

A. Deltuva and A. C. Fonseca

Centro de Física Nuclear da Universidade de Lisboa, P-1649-003 Lisboa, Portugal
(Received 10 November 2006; published 18 April 2007)

The four-body equations of Alt, Grassberger, and Sandhas are solved, for the first time, for proton- ^3He scattering including the Coulomb interaction between the three protons using the method of screening and renormalization as was done recently for proton-deuteron scattering. Various realistic two-nucleon potentials are used. Large Coulomb effects are seen on all observables. Comparison with data at different energies shows large deviations in the proton analyzing power but quite reasonable agreement in other observables. The effect of the nucleon-nucleon magnetic moment interaction and correlations between p - d and p - ^3He analyzing powers are studied.

DOI: [10.1103/PhysRevLett.98.162502](https://doi.org/10.1103/PhysRevLett.98.162502)

PACS numbers: 21.30.-x, 21.45.+v, 24.70.+s, 25.10.+s

Modern calculations of light nuclear systems $A \leq 12$ are essential to our understanding of the force models that have been developed to describe how nucleons interact at low energies [1,2]. Of these nuclear systems, the four-nucleon ($4N$) system is particularly important because it gives rise, experimentally, to the simplest set of nuclear reactions that shows the complexity of heavier systems and the Coulomb interaction manifests itself in new ways relative to what is observed in the three-nucleon ($3N$) system. Theoretically it is also important because with powerful numerical techniques and fast computers one can calculate not only bound state properties [3] but also scattering observables [4–10] for a number of elastic, transfer, and breakup reactions that place new challenges to our understanding of the underlying force models. The importance of scattering calculations also has to do with the possibility to probe states in the continuum associated with specific resonances, states of higher angular momentum than corresponding bound states, effects that depend on the spin orientation of the projectile and/or target, and threshold effects on the observables, among others.

While the three-nucleon system has been extensively studied [11,12] through neutron-deuteron (n - d) and proton-deuteron (p - d) elastic scattering and breakup experiments, exact calculations using realistic force models as well as interactions derived from effective field theory were restricted, for a long time, to the n - d system due to limitations in including the Coulomb force in the description of p - d scattering beyond low-energy p - $d \rightarrow p$ - d and p - $d \leftrightarrow \gamma^3\text{He}$ calculations [13,14] in the framework of the variational hyperspherical approach. The situation has now changed due to the work of Refs. [15,16] where calculations of p - $d \rightarrow p$ - d , p - $d \rightarrow ppn$, p - $d \leftrightarrow \gamma^3\text{He}$, $\gamma^3\text{He} \rightarrow ppn$, $e^3\text{He} \rightarrow e'p$ - d , and $e^3\text{He} \rightarrow e'ppn$ were performed at energies ranging from 1 MeV in the center of mass (c.m.) system to the pion production threshold. The work is based on the solution of the momentum-space Alt, Grassberger, and Sandhas (AGS) equations [17] together with the screening and renormalization approach [18–20] for the Coulomb interaction leading to the results of observables

that are independent of the screening radius, provided it is sufficiently large.

In the present Letter for the first time we extend the method of Refs. [15,16] to the p - ^3He elastic scattering using the four-body AGS equations [21]. The aim is to bring the $4N$ scattering problem to the same level of understanding in terms of the underlying two-nucleon ($2N$) forces as already exists for $3N$, which means that calculations are carried out without approximations on the $2N$ transition matrix (t matrix) like in Ref. [6] or limitations on the choice of basis functions as in Refs. [22,23]. Therefore, after partial-wave decomposition, the AGS equations are three-variable integral equations that are solved numerically without any approximations beyond the usual discretization of continuum variables on a finite momentum mesh. The results we present here are converged *vis-à-vis* number of partial waves and momentum meshpoints as well as the value of the screening radius of the Coulomb potential. These calculations are also an extension to p - ^3He of the work already developed for n - ^3H [24] and were presented for the first time in Ref. [25]. Our work follows the work of Refs. [7,22,23], but with greater number of $2N$, $3N$, and $4N$ partial waves in order to get fully converged results for the spin observables and with various $2N$ potentials. The advantage of the present work is that it is easier to extend to inelastic reactions and to use with nonlocal interactions.

Our description of $4N$ scattering is based on the symmetrized four-body AGS equations given in Ref. [24] where the solution technique is discussed in detail. In order to include the Coulomb interaction we follow the methodology of Refs. [15,16] and add to the nuclear pp potential the screened Coulomb one w_R that, in configuration space, is given by

$$w_R(r) = w(r)e^{-(r/R)^n}, \quad (1)$$

where $w(r) = \alpha_e/r$ is the true Coulomb potential, $\alpha_e \simeq 1/137$ is the fine structure constant, and n controls the smoothness of the screening; $n = 4$ is the optimal value

which ensures that $w_R(r)$ approximates well $w(r)$ for $r < R$ and simultaneously vanishes rapidly for $r > R$, providing a comparatively fast convergence of the partial-wave expansion. The screening radius R must be considerably larger than the range of the strong interaction but from the point of view of scattering theory w_R is still of short range. Therefore, the equations of Ref. [24] become R dependent. The transition operators $\mathcal{U}_{(R)}^{\alpha\beta}$, where $\alpha(\beta) = 1$ and 2 corresponds to initial/final $1 + 3$ and $2 + 2$ two-cluster states, respectively, satisfy the symmetrized AGS equations

$$\mathcal{U}_{(R)}^{11} = -(G_0 t^{(R)} G_0)^{-1} P_{34} - P_{34} U_{(R)}^1 G_0 t^{(R)} G_0 \mathcal{U}_{(R)}^{11} + U_{(R)}^2 G_0 t^{(R)} G_0 \mathcal{U}_{(R)}^{21}, \quad (2a)$$

$$\mathcal{U}_{(R)}^{21} = (G_0 t^{(R)} G_0)^{-1} (1 - P_{34}) + (1 - P_{34}) U_{(R)}^1 G_0 t^{(R)} G_0 \mathcal{U}_{(R)}^{11}. \quad (2b)$$

Here G_0 is the four free particle Green's function and $t^{(R)}$ the two-nucleon t matrix derived from nuclear potential plus screened Coulomb between pp pairs. The operators $U_{(R)}^\alpha$ obtained from

$$U_{(R)}^\alpha = P_\alpha G_0^{-1} + P_\alpha t^{(R)} G_0 U_{(R)}^\alpha, \quad (3a)$$

$$P_1 = P_{12} P_{23} + P_{13} P_{23}, \quad (3b)$$

$$P_2 = P_{13} P_{24}, \quad (3c)$$

are the symmetrized AGS operators for the $1 + (3)$ and $(2) + (2)$ subsystems and P_{ij} is the permutation operator of particles i and j . Defining the initial/final $1 + (3)$ and $(2) + (2)$ states with relative two-body momentum \mathbf{p}

$$|\phi_\alpha^{(R)}(\mathbf{p})\rangle = G_0 t^{(R)} P_\alpha |\phi_\alpha^{(R)}(\mathbf{p})\rangle, \quad (4)$$

the amplitudes for $1 + 3 \rightarrow 1 + 3$ and $1 + 3 \rightarrow 2 + 2$ are obtained as $\langle \mathbf{p}_f | T_{(R)}^{\alpha\beta} | \mathbf{p}_i \rangle = S_{\alpha\beta} \langle \phi_\alpha^{(R)}(\mathbf{p}_f) | \mathcal{U}_{(R)}^{\alpha\beta} | \phi_\beta^{(R)}(\mathbf{p}_i) \rangle$ with $S_{11} = 3$ and $S_{21} = \sqrt{3}$.

In close analogy with p - d elastic scattering, the full scattering amplitude, when calculated between initial and final p - ^3He states, may be decomposed as follows

$$T_{(R)}^{11} = t_R^{\text{c.m.}} + [T_{(R)}^{11} - t_R^{\text{c.m.}}], \quad (5)$$

with the long-range part $t_R^{\text{c.m.}}$ being the two-body t matrix derived from the screened Coulomb potential of the form (1) between the proton and the c.m. of ^3He and the remaining Coulomb-distorted short-range part $[T_{(R)}^{11} - t_R^{\text{c.m.}}]$ as demonstrated in Refs. [20,26]. Applying the renormalization procedure, i.e., multiplying both sides of Eq. (4) by the renormalization factor Z_R^{-1} [15,20], in the $R \rightarrow \infty$ limit, yields the full $1 + 3 \rightarrow 1 + 3$ transition amplitude in the presence of Coulomb

$$\langle \mathbf{p}_f | T^{11} | \mathbf{p}_i \rangle = \langle \mathbf{p}_f | t_C^{\text{c.m.}} | \mathbf{p}_i \rangle + \lim_{R \rightarrow \infty} \{ \langle \mathbf{p}_f | [T_{(R)}^{11} - t_R^{\text{c.m.}}] | \mathbf{p}_i \rangle Z_R^{-1} \}, \quad (6)$$

where the $Z_R^{-1} \langle \mathbf{p}_f | t_R^{\text{c.m.}} | \mathbf{p}_i \rangle$ converges (in general, as a

distribution) to the exact Coulomb amplitude $\langle \mathbf{p}_f | t_C^{\text{c.m.}} | \mathbf{p}_i \rangle$ between the proton and the c.m. of the ^3He nucleus, and therefore is replaced by it. The renormalization factor is employed in the partial-wave dependent form as in Ref. [15]

$$Z_R = e^{-2i(\sigma_L - \eta_{LR})} \quad (7)$$

with the diverging screened Coulomb p - ^3He phase shift η_{LR} corresponding to standard boundary conditions and the proper Coulomb one σ_L referring to the logarithmically distorted proper Coulomb boundary conditions. The second term in Eq. (6), after renormalization by Z_R^{-1} , represents the Coulomb-modified nuclear short-range amplitude. It has to be calculated numerically, but, due to its short-range nature, the $R \rightarrow \infty$ limit is reached with sufficient accuracy at finite screening radii R . As in p - d elastic scattering [15] one needs larger values of R for decreasing proton energies, making the convergence of the results more difficult to reach. Nevertheless, for $E_p > 2$ MeV the method leads to very precise results as we demonstrate in Fig. 1 for the differential cross section $d\sigma/d\Omega$, proton analyzing power A_y , and p - ^3He spin correlation coefficient

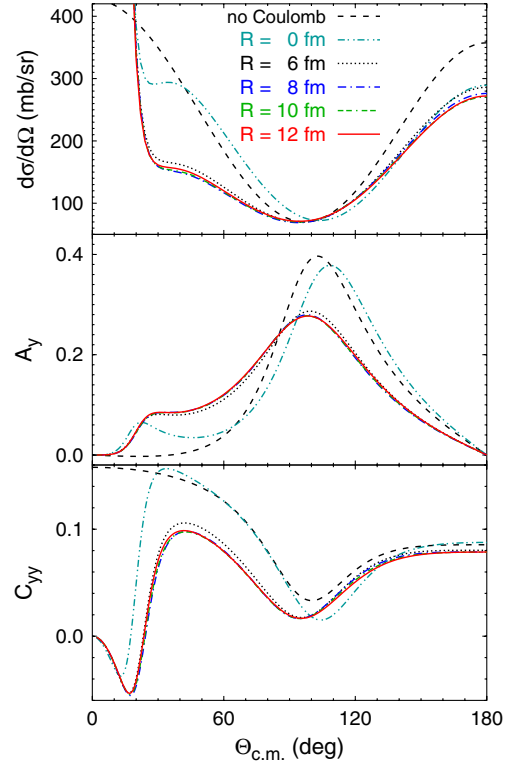


FIG. 1 (color online). Convergence of the p - ^3He scattering observables with screening radius R . Results for the differential cross section, proton analyzing power A_y , and p - ^3He spin correlation coefficient C_{yy} at 4 MeV proton lab energy obtained with screening radius $R = 0$ fm (dashed-double-dotted curves), 6 fm (dotted curves), 8 fm (dashed-dotted curves), 10 fm (double-dashed-dotted curves), and 12 fm (solid curves) are compared. Results without Coulomb (dashed curves) are given as reference for the size of the Coulomb effect.

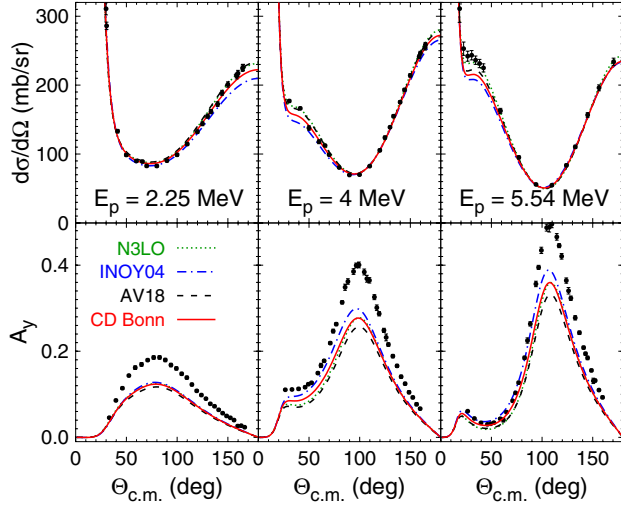


FIG. 2 (color online). The differential cross section and proton analyzing power A_y at 2.25, 4.0, and 5.54 MeV proton lab energy. Results including the Coulomb interaction obtained with potentials CD Bonn (solid curves), AV18 (dashed curves), INOY04 (dashed-dotted curves), and N3LO (dotted curves) are compared. The data are from Refs. [22,32,33].

C_{yy} at proton lab energy $E_p = 4$ MeV. The observables are shown as functions of the c.m. scattering angle. Fully converged results are obtained with $R = 12$ fm, but already $R = 8$ and 10 fm results are very close to them. The calculations include isospin-singlet $2N$ partial waves with total angular momentum $I \leq 4$ and isospin-triplet $2N$ partial waves with orbital angular momentum $l_x \leq 7$, $3N$ partial waves with spectator orbital angular momentum $l_y \leq 7$ and total angular momentum $J \leq \frac{13}{2}$, $4N$ partial waves with $1 + 3$ and $2 + 2$ orbital angular momentum $l_z \leq 7$, and all initial/final p - ^3He states with orbital angular momentum $L \leq 3$. The charge-dependent (CD) Bonn potential [27] is used. The effect of Coulomb is large in the whole angular region, particularly for A_y where it reduces the magnitude of the maximum. The $R = 0$ fm curve corresponds to the so-called Doleschall approximation which clearly fails to reproduce the full Coulomb effect.

In Figs. 2–4 we compare the results of our calculations with data for a number of observables at $E_p = 2.25$, 4.0, and 5.54 MeV. In addition to CD Bonn we use AV18 [28], inside-nonlocal outside-Yukawa (INOY04) potential by Doleschall [9,29] and the one derived from chiral perturbation theory at next-to-next-to-next-to-leading order (N3LO) [30]. The ^3He binding energy (BE) calculated with AV18, N3LO, CD Bonn, and INOY04 potentials is 6.92, 7.13, 7.26, and 7.73 MeV, respectively; the experimental value is 7.72 MeV. As in n - ^3H scattering [24], p - ^3He observables depend on the choice of potential; predictions with N3LO and AV18 agree best with the cross section data but it is INOY04 that provides the highest A_y at the peak. If one considers AV18, CD Bonn, and INOY04 potentials alone, one might be tempted to conclude about a possible correlation between observables and ^3He BE.

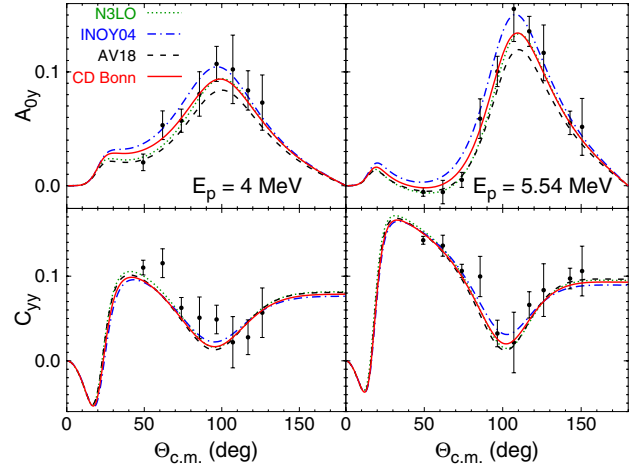


FIG. 3 (color online). ^3He target analyzing power A_{0y} and spin correlation coefficient C_{yy} at 4.0 and 5.54 MeV proton lab energy. Curves as in Fig. 2. The data are from Ref. [33].

Nevertheless, as discussed in Ref. [24], N3LO, for reasons not yet fully understood, breaks this correlation in the considered energy region. As found in Ref. [24], $4N$ S -wave phase shifts correlate with the $3N$ BE [24] but as the energy increases $4N$ P waves become very important as well and behave differently depending on the choice of potential. Therefore, correlations between p - ^3He observables and ^3He BE cannot be established easily without further studies, e.g., inclusion of a $3N$ force.

As shown in Figs. 3 and 4 ^3He target analyzing power A_{0y} and p - ^3He spin correlation coefficients C_{jk} are described quite satisfactorily. This updates the findings of Ref. [22] based on AV18 potential where significant discrepancies were observed for A_{0y} and C_{yy} . However, the proton analyzing power is clearly underestimated by all potentials. In contrast to low-energy p - d elastic scattering where variations of the $2N$ interaction at the maximum of

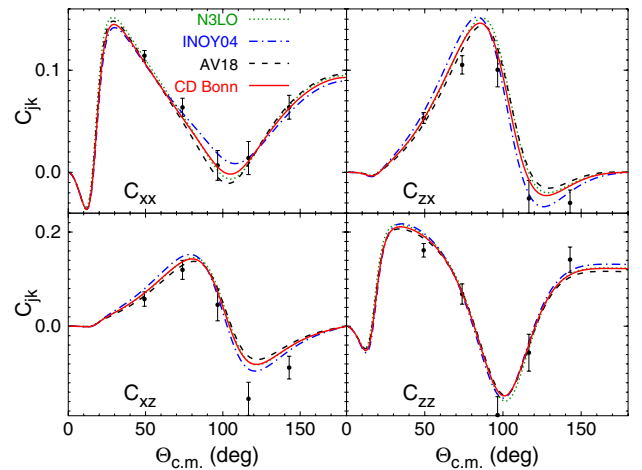


FIG. 4 (color online). p - ^3He spin correlation coefficients at 5.54 MeV proton lab energy. Curves as in Fig. 2. The experimental data are from Ref. [33].

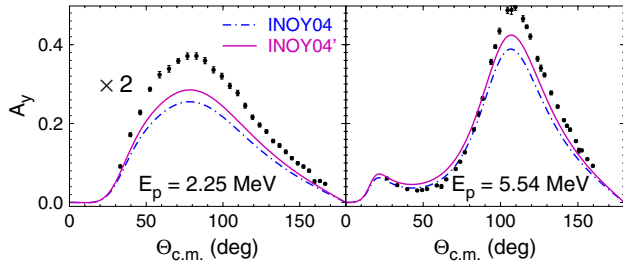


FIG. 5 (color online). Proton analyzing power A_y at 2.25 and 5.54 MeV proton lab energy. Results for the potentials INOY04 (dashed-dotted curves) and INOY04' (solid curves) are compared. The experimental data are from Refs. [22,33].

A_y lead to 10% fluctuations, here we get 15%, which means that the $4N$ system is more sensitive to off-shell differences of the $2N$ force than the $3N$ system.

In Fig. 5 we compare A_y for potential INOY04 and its version INOY04' [9,29] with modified $2N$ $3P_I$ wave parameters such that it provides quite satisfactory description of A_y in low-energy n - d and p - d scattering at the cost of being inconsistent with the $2N$ data. However, for p - ^3He A_y disagreement with data still persists.

In Fig. 6 we investigate the effect of $2N$ magnetic moment (MM) interaction. As for p - d scattering [31] it is most visible for A_y at low energy where at $E_p = 2.25$ MeV it gives rise to a 5.3% increase towards the data. At 4 MeV the MM interaction effect is reduced to 2.7%.

In conclusion, we have been able to obtain *ab initio* four-nucleon results for p - ^3He scattering that include the Coulomb interaction between the protons for different realistic local and nonlocal $2N$ interactions. The reliability of the screening and renormalization approach is demonstrated. The calculations describe existing data quite well except proton A_y where there is 25%–40% discrepancy at the peak. We find that $4N$ observables are more sensitive than $3N$ observables to off-shell changes in the $2N$ interaction, and that curing A_y in low energy $3N$ scattering through changes in the $2N$ $3P_I$ partial waves still gives rise to a p - ^3He A_y deficiency. A visible effect of $2N$ magnetic moment interaction is found for A_y at very low energy.

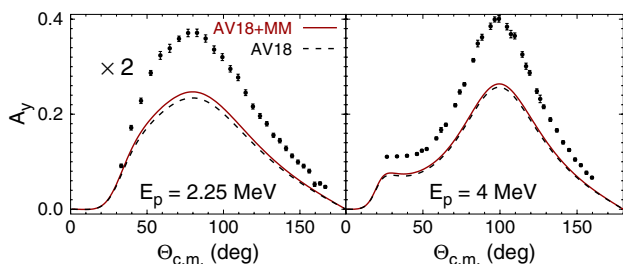


FIG. 6 (color online). Proton analyzing power A_y at $E_p = 2.25$ and 4.0 MeV. Results for AV18 potential without (dashed curves) and with (solid curves) magnetic moment interaction are compared. The data are from Refs. [22,33].

A. D. is supported by Fundação para a Ciência e a Tecnologia (FCT) Grant No. SFRH/BPD/14801/2003 and A. C. F. in part by FCT Grant No. POCTI/ISFL/2/275.

- [1] S. C. Pieper *et al.*, Phys. Rev. C **64**, 014001 (2001).
- [2] S. C. Pieper, K. Varga, and R. B. Wiringa, Phys. Rev. C **66**, 044310 (2002).
- [3] A. Nogga *et al.*, Phys. Rev. C **65**, 054003 (2002).
- [4] M. Viviani, S. Rosati, and A. Kievsky, Phys. Rev. Lett. **81**, 1580 (1998).
- [5] F. Cieselski, J. Carbonell, and C. Gignoux, Phys. Lett. B **447**, 199 (1999); J. Carbonell, Few-Body Syst. Suppl. **12**, 439 (2000).
- [6] A. C. Fonseca, Phys. Rev. Lett. **83**, 4021 (1999).
- [7] M. Viviani *et al.*, Phys. Rev. Lett. **86**, 3739 (2001).
- [8] A. C. Fonseca, G. Hale, and J. Haidenbauer, Few-Body Syst. **31**, 139 (2002).
- [9] R. Lazauskas and J. Carbonell, Phys. Rev. C **70**, 044002 (2004).
- [10] R. Lazauskas *et al.*, Phys. Rev. C **71**, 034004 (2005).
- [11] W. Glöckle *et al.*, Phys. Rep. **274**, 107 (1996).
- [12] J. Golak *et al.*, Phys. Rep. **415**, 89 (2005).
- [13] A. Kievsky, M. Viviani, and S. Rosati, Phys. Rev. C **64**, 024002 (2001).
- [14] M. Viviani *et al.*, Phys. Rev. C **61**, 064001 (2000).
- [15] A. Deltuva, A. C. Fonseca, and P. U. Sauer, Phys. Rev. C **71**, 054005 (2005); **72**, 054004 (2005).
- [16] A. Deltuva, A. C. Fonseca, and P. U. Sauer, Phys. Rev. Lett. **95**, 092301 (2005).
- [17] E. O. Alt, P. Grassberger, and W. Sandhas, Nucl. Phys. **B2**, 167 (1967).
- [18] J. R. Taylor, Nuovo Cimento B **23**, 313 (1974); M. D. Semon and J. R. Taylor, Nuovo Cimento A **26**, 48 (1975).
- [19] E. O. Alt, W. Sandhas, and H. Ziegelmann, Phys. Rev. C **17**, 1981 (1978).
- [20] E. O. Alt and W. Sandhas, Phys. Rev. C **21**, 1733 (1980).
- [21] P. Grassberger and W. Sandhas, Nucl. Phys. **B2**, 181 (1967); E. O. Alt, P. Grassberger, and W. Sandhas, JINR Report No. E4-6688, 1972.
- [22] B. M. Fisher *et al.*, Phys. Rev. C **74**, 034001 (2006).
- [23] B. Pfitzinger, H. M. Hofmann, and G. M. Hale, Phys. Rev. C **64**, 044003 (2001).
- [24] A. Deltuva and A. C. Fonseca, Phys. Rev. C **75**, 014005 (2007).
- [25] A. Deltuva and A. C. Fonseca, nucl-th/0611013.
- [26] A. Deltuva and A. C. Fonseca (to be published).
- [27] R. Machleidt, Phys. Rev. C **63**, 024001 (2001).
- [28] R. B. Wiringa, V. G. J. Stoks, and R. Schiavilla, Phys. Rev. C **51**, 38 (1995).
- [29] P. Doleschall, Phys. Rev. C **69**, 054001 (2004).
- [30] D. R. Entem and R. Machleidt, Phys. Rev. C **68**, 041001(R) (2003).
- [31] A. Kievsky, M. Viviani, and L. E. Marcucci, Phys. Rev. C **69**, 014002 (2004).
- [32] D. G. McDonald, W. Haerberli, and L. W. Morrow, Phys. Rev. **133**, B1178 (1964).
- [33] M. T. Alley and L. D. Knutson, Phys. Rev. C **48**, 1890 (1993).